

This paper is an extended version of a contribution presented
at the [Graphicon 2025 conference](#).

Visual Processing of the Results of Supersonic Flow Around a Delta Wing

T.V. Konstantinovskaya¹, V.E. Borisov², A.E. Lutsky³

Keldysh Institute of Applied Mathematics RAS, Moscow, Russia

¹ ORCID: 0000-0002-1127-503X, konstantinovskaya@kiam.ru

² ORCID: 0000-0003-4448-7474, borisov@keldysh.ru

³ ORCID: 0000-0002-4442-0571, allutsky@yandex.ru

Abstract

The paper considers the problem of visual processing of the numerical simulation results of vortex structures in supersonic flow around delta wing. The methods of visual processing of the obtained structures using various methods of scientific identification of vortex structures and visualization of vortex flows are shown. The obtained results are compared for different incoming flow Mach numbers. The delta wing under consideration had an attack angle of 14°. Numerical simulations were performed on the hybrid supercomputer system K-60 at the Supercomputer Centre of Collective Usage of KIAM RAS.

Keywords: Flow around delta wing, vortex, vortex structures identification, scientific visualization.

1. Introduction

The lack of a strict, universally applicable definition of "vortex" poses a serious problem in aerodynamics, affecting our ability to quantify, model, and predict complex flow phenomena. Despite the fact that the concept of a vortex is intuitive – it is an area of swirling fluid motion – it turned out to be difficult to translate this intuition into an accurate mathematical or physical criterion. This ambiguity leads to several key problems.

Various methods for identifying vortices (for example, the Q criterion, the λ_2 -criterion, and the minimum pressure) often give contradictory results, while demonstrating their subjectivity. What one method defines as a vortex, the other may not be able to determine, especially in complex, turbulent flows or flows with strong shear layers [1]. This subjectivity makes it difficult to compare the results of various studies and hinders the development of reliable automated algorithms for detecting vortices.

Without a clear definition, it becomes difficult to quantify the properties of a vortex such as strength, size, and circulation. This limits the possibilities for accurate modeling of vortex flows, predicting their impact on aerodynamic characteristics (for example, lift, drag, stability) and developing effective flow control strategies.

The lack of a precise definition affects the development and validation of computational fluid dynamics (CFD) models. Different turbulence models and numerical schemes can lead to varying vortex structures in simulations, making it difficult to assess the accuracy and reliability of the results. Furthermore, without a consistent definition, it's hard to objectively compare simulations with experimental data.

Delta-shaped or triangular wings have been actively used in aviation since the 1950s with the development of high-speed vehicles, where they have become widely used. Such wings are also used in the field of aerospace technology.

Today, interest in triangular wings is increasing not only in aviation, due to the fact that travel speeds are of great importance in the modern world, but also in the aerospace sector in the context of the development of reusable space systems.

The widespread use of triangular wings has contributed to the active study of their aerodynamic characteristics both in our country and abroad.

Careful study of the aerodynamic characteristics of high-speed vehicles flight is crucial for their designing and building. One of the main tasks is to study the vortex structures that inevitably accompany supersonic flow around a triangular wing.

Methods of scientific identification and visualization of vortex structures can be effectively used to process and analyze the data obtained during numerical and experimental modeling. These methods provide tools not only for visualizing flows, but also for their in-depth analysis [2-6].

This paper presents the visualization results of a numerical study of supersonic flow around delta wing. A comparison of the results for the free-stream Mach numbers $M_\infty = 2$ and $M_\infty = 3$ was effectuated. The formation of vortex structures on the edge and surface of the wing is shown. The authors used various methods for identifying and visualizing vortex flows, in particular, the Liutex criterion [6-9], which belongs to the third generation of such methods. The URANS approach with the SA turbulence model was used for numerical calculations. The simulations were performed on the multiprocessor hybrid system K-60 at the Supercomputer Centre of Collective Usage of KIAM RAS [10].

2. Problem statement

The supersonic flow around a triangular wing was studied. The wing had sharp edges, a sweep of 78° , a half-span of 0.1118 m, a root chord of 0.526 m, and an angle of attack of $\alpha = 14^\circ$. Two values of the incoming flow Mach number M_∞ were considered $M_\infty = 2$ and 3. The Reynolds number in both cases was given by $ReL = 1 \times 10^7$ (L is the characteristic length of the dimensionalization of the computational model, here $L = 1$ m). Figure 1 shows a scheme of the computational domain. An unstructured grid containing 7315200 curvilinear hexahedron cells was used.

The flow was considered at a distance of up to 2.8 of the wing root chord downstream from the trailing edge of the wing.

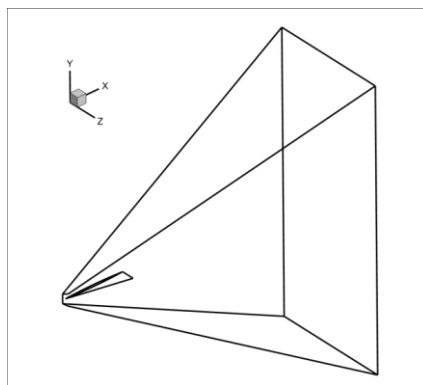


Figure 1: Simulation domain, triangle wing position

3. Numerical simulation

An associated Cartesian coordinate system was defined in the computational domain, the origin of which coincides with the vertex of the triangular wing. The O_x axis is directed along the root chord of the wing, and the xOy plane coincides with the plane of symmetry. The O_z

axis is perpendicular to the plane of symmetry. The median surface of the wing lies in the $z = 0$ plane.

The numerical data were obtained using the author's ARES software package [11], developed at the Keldysh Institute of Applied Mathematics of the Russian Academy of Sciences.

A system of unsteady Reynolds and Favre averaged Navier-Stokes equations (URANS) was used to simulate the three-dimensional turbulent flow of a compressible gas. The one-parameter Spalart-Allmaras (SA) turbulence model was applied in a modification for compressible flows [12]. The initial and boundary conditions were set in a standard way.

The approximation of the model equations in the spatial direction was performed using the finite volume method with the TVD second-order accurate reconstruction scheme.

Both explicit and implicit schemes were used for the temporal approximation of the equations. A detailed description of the numerical method used can be found in [13].

The numerical simulations were performed on the hybrid supercomputer system K-60 [14] at the Supercomputer Centre of Collective Usage of KIAM RAS [10].

4. Vortex system visualization

For visual representation and analysis of vortex structures, it is necessary to identify and distinguish them from the rest of the flow. As already mentioned, at the moment there is no single mathematically clear definition of a vortex, which leads to a variety of approaches and methods for its identification. In this regard, further work continues on the search and development of new and optimal methods for the identification and visualization of vortex structures for their study [15-17]. However, this problem is not among the interests of the authors, the authors are engaged in the practical application of these methods for data analysis.

For the purpose of vortex structures identification in the flow, a special separate module was developed inside the author's software package ARES, which allows to identify and analyze vortex structures on hexagonal grids in the post-processing mode of data processing. It implements some classical methods of scientific identification and visualization, such as the λ_2 , Q -criterion, and others [18, 19]. The module also contains the Liutex method of scientific visualization, one of the latest and most modern criteria for the identification of vortex structures, belonging to the third generation of such methods. The mentioned post-processing module generates the output data in the format of the Tecplot software package.

In this paper, the results of numerical calculations and their analysis are visualized using various methods for identifying and visualizing vortex structures. In particular, approaches are used with the direct use of gradients of the basic and derived gas dynamic properties of the flow.

5. Simulation results and visualization of vortex structures

This section of the article presents the obtained results of the numerical simulations. Figure 2 shows a general view of the vortex structures formed in supersonic flow around a delta wing. To visualize the flow results in Figure 2, pressure isosurfaces P are used, allowing the main vortices to be clearly distinguished as longitudinal structures. The isosurfaces are shown for three pressure values: 0.2, 0.25, and 0.3, the transparency property is used.

In the problem statement under consideration, the vortex system forms on the leeward side of a delta wing. It is quite complex and consists of the following main elements. There are a vortex at the leading edge (first vortex), a main vortex, and a secondary vortex (Fig. 3). Figure 3 shows the distribution of the x -th component of the rotor velocity (vorticity) $XVorticity$ and the streamlines in the cross-section $x = 0.45$, intersecting the wing closer to the trailing edge, $M_\infty = 2$ on the left, $M_\infty = 3$ on the right. The secondary vortex is caused by boundary layer separation (marked in red in Fig. 3), which occurs due to an unfavorable pressure gradient, namely, an increase in pressure toward the leading edge. The secondary vortex rotates in a direction opposite to that of the main vortex.

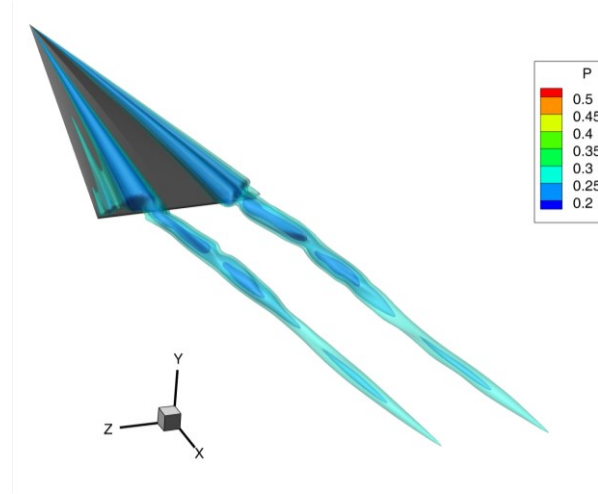


Figure 2: General view of obtained numerically data flow, case $M_\infty = 2$

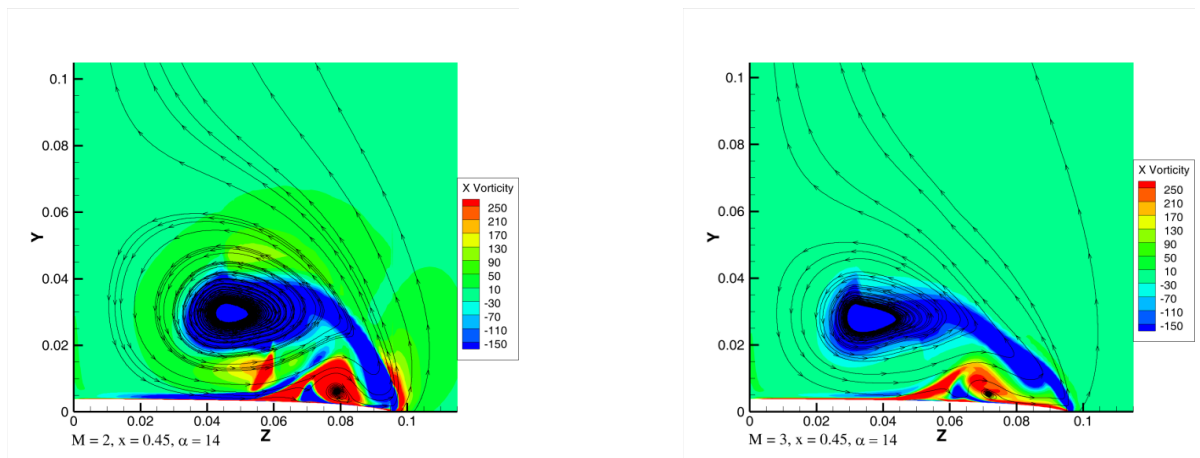


Figure 3: *XVorticity* distribution and streamtraces projected onto the cross-section $x = 0.45$: $M_\infty = 2$ (left) and $M_\infty = 3$ (right).

Using the longitudinal vorticity *XVorticity* allows us to demonstrate the direction of rotation of the identified longitudinal vortex structures (Fig. 3, Fig. 4). Fig. 4 illustrates the application of the λ_2 -criterion, showing the isosurfaces of $\lambda_2 = -4000$ for the considered configuration at the Mach numbers of the incoming flow: a) $M_\infty = 2$ and b) $M_\infty = 3$. At the same time, they are colored with the longitudinal component of the vorticity vector, which really gives an idea not only about the presence and position of vortex structures, but also about the direction of their rotation. In Fig. 4, the structure-forming vortices (on the leading edge, secondary, main) are clearly distinguishable in space. When using the same parameter values, in the case of the Mach number $M_\infty = 3$, the main vortex is visually represented noticeably further away than in the case of the Mach number $M_\infty = 2$. In other words, it can be concluded that in the geometry considered in the near region of the wake, the greater the Mach number of the incoming flow, the stronger the main vortex.

Figure 5 shows the axes of the structure-forming vortices: on the leading edge, the main and secondary, they were obtained by analyzing various flow properties. Namely, the axis of the main vortex is determined by the minimum pressure, the axis of the secondary vortex is determined by the minimum density, and the vortex on the leading edge is determined by the maximum vorticity and the Liutex criterion.

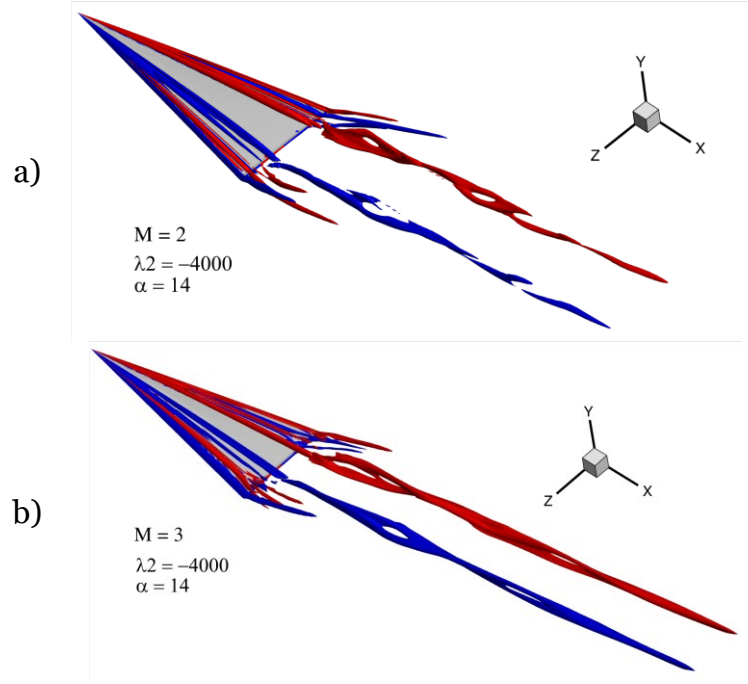


Figure 4: Vortex structures visualization using λ_2 -criteria and *XVorticity*: isosurfaces of $\lambda_2 = -3000$

The combination of the vorticity magnitude and the λ_2 -criterion for visual representation of the flow properties and the position of vortex structures is shown in Fig. 6, which shows the distribution of the corresponding parameters in four cross-sections for the following values of x : $x = 0.4$, $x = 0.75$, $x = 1.0$ and $x = 1.4$. It can be seen that the methods give consistent the results.

It is found that at some distance from the wing, its vortex system merges into one longitudinal vortex structure, which is clearly distinguishable and extends up to the boundaries of the region under consideration (Fig. 5 – Fig. 7).

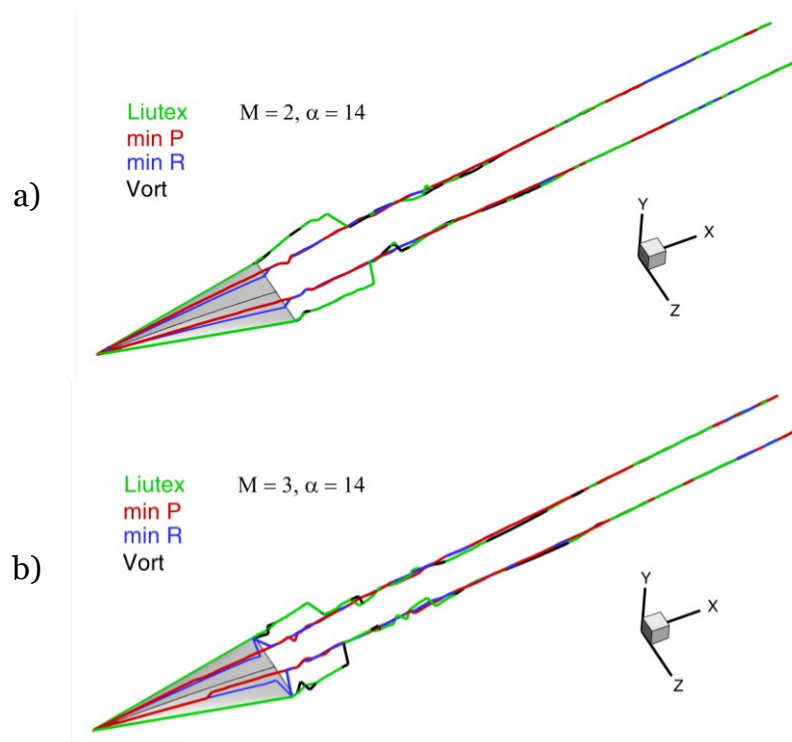


Figure 5: Vortex axes determination: first (on the leading edge), main and secondary. $M_\infty = 2$ (a), $M_\infty = 3$ (b), $\alpha = 14^\circ$

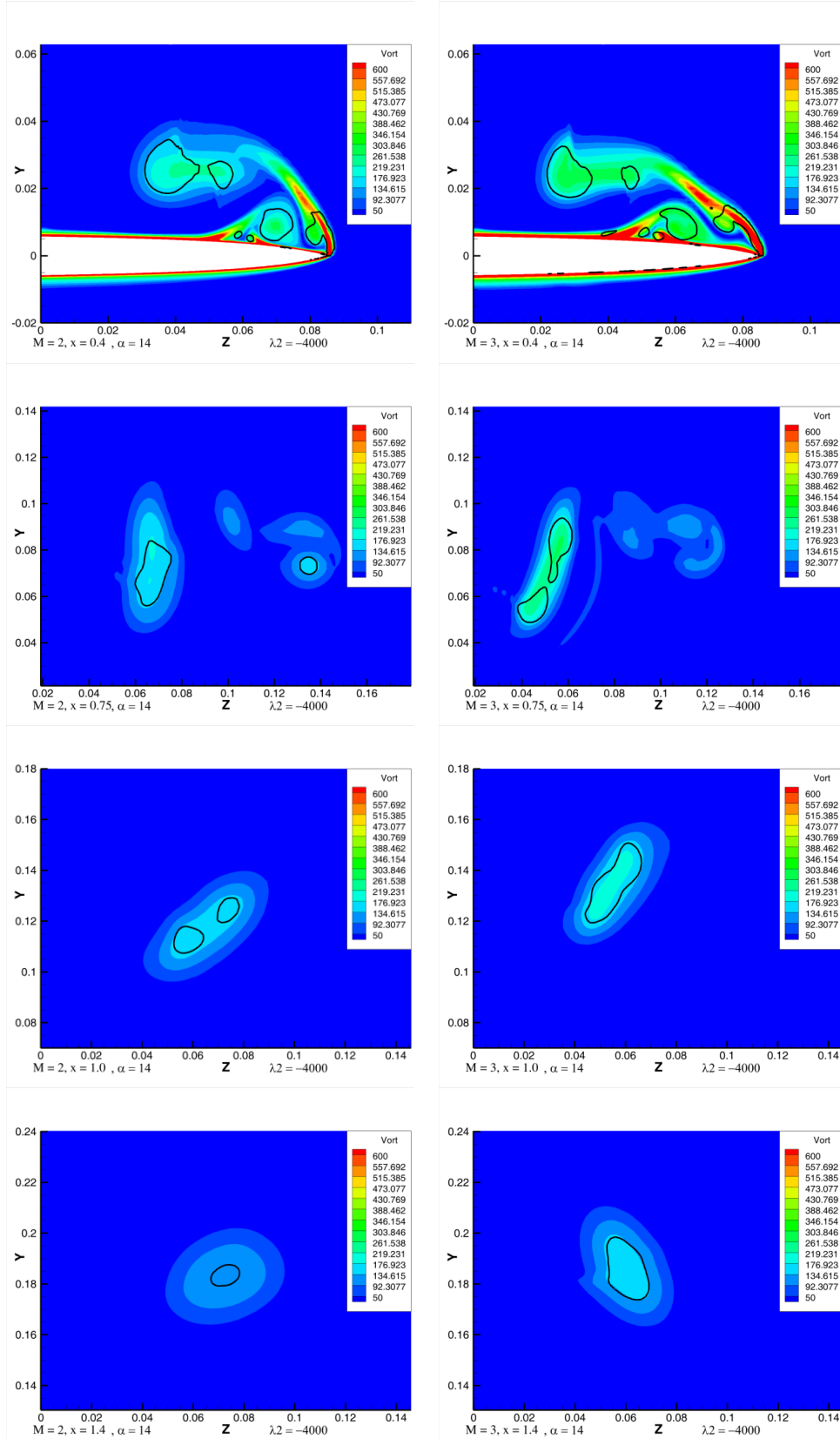


Figure 6: Visualization of vortex structures using the vorticity magnitudes $Vort$ and the λ_2 -criterion: cross-sections are shown at $x = \text{const}$ ($x = 0.4, 0.75, 1.0, 1.4$), isosurfaces of $\lambda_2 = -4000$ are shown by a black line.

Figure 7 shows the application of the Q criterion. The isosurfaces of $Q = 500$ are shown, which are colored by the pressure values P . The case of a flow with the incoming flow Mach number $M_\infty = 2$ is shown above, and for $M_\infty = 3$ is shown below. Adding pressure values

makes it possible to see the nuances of the effect of a tail shock wave and pressure changes in a vortex system in three-dimensional space. After interacting with the tail shock wave, the secondary vortex and the vortex on the leading edge dissipate rapidly, merging with the main vortex into a single longitudinal vortex structure.

Thus, from the above results, it can be noted that various methods of identification and visualization of vortex structures can be used both separately and in combination with each other to achieve more accurate and informative identification and visualization of vortex structures in various flows, while allowing for complementary results and deeper data analysis.

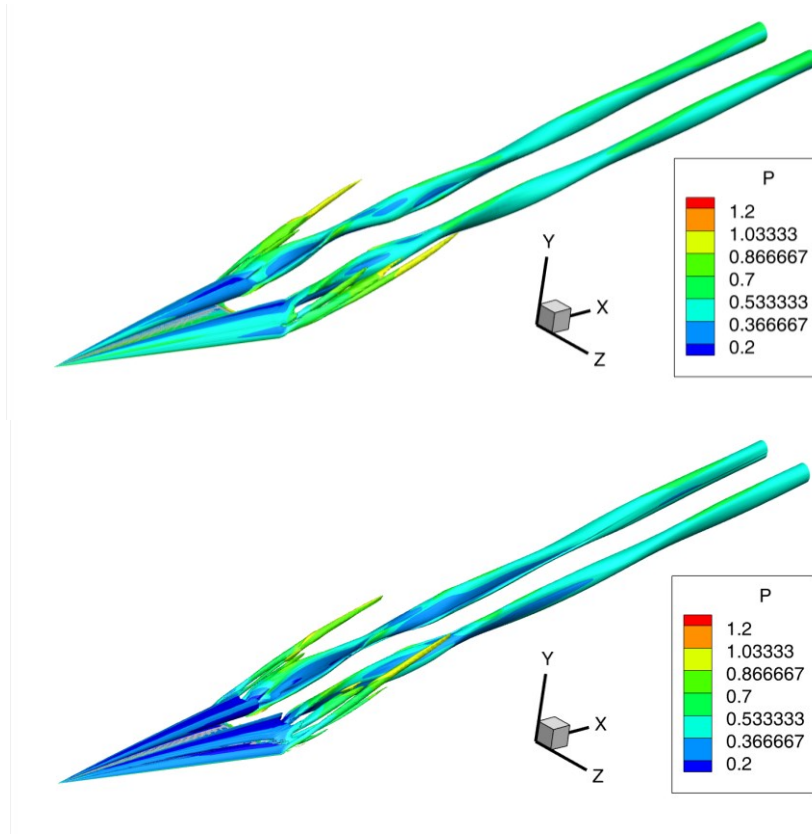


Figure 7: Vortex structures visualization using an isosurfaces of Q criteria ($Q = 500$) with the pressure P plotted on top of them, $M_\infty = 2$ (top) and $M_\infty = 3$ (bottom)

6. Conclusion

The paper considers results of numerical simulations of supersonic flow around a triangular wing. Two values of the incoming flow Mach number are considered: $M_\infty = 2$ and $M_\infty = 3$. The application of various methods and approaches to scientific visualization of vortex structures in the obtained flows, as well as the use of scientific visualization for data analysis, is demonstrated. Numerical simulations were performed using the author's software package ARES on the supercomputer K-60 at the Supercomputer Centre of Collective Usage of KIAM of the Russian Academy of Sciences.

It is found that during supersonic flow around a triangular wing in the considered configuration, its vortex system consists of three basic structures: a first vortex (on the leading edge), a secondary and a main one. At the same time, for a larger Mach number, the main vortex is located closer to the surface of the wing and to its root chord.

At some distance downstream the trailing edge of the wing, these vortex structures merge into one, forming one vortex that extends all the way to the end of the considered area. At the same time, for a larger Mach number, this merging occurs in a shorter area.

It is noted that the use of longitudinal vorticity makes it possible to obtain the direction of rotation of the longitudinal vortex structures.

Using the example of the considered problem and the effectuated comparison, it is shown how a comprehensive analysis of numerical data can be implemented by combining various methods and approaches to the identification and visualization of vortex structures.

References

1. Kolář V., Šístek J. Disappearing vortex problem in vortex identification: Non-existence for selected criteria // *Physics of Fluids*. 2022. 34, 071704. DOI: 10.1063/5.0099046
2. Yang Wen-Jei. Handbook of flow visualization. CRC Press; 2nd edition. 2001. 724 p.
3. Kolář V. Vortex identification: New requirements and limitations // *International Journal of Heat and Fluid Flow*. 2007. **28** 4, pp. 638-652. DOI: 10.1016/j.ijheatfluidflow.2007.03.004
4. Volkov K.N. Methods of visualization of vortex flows in computational gas dynamics and their application in solving applied problems // *Scientific and Technical Bulletin of Information Technologies, Mechanics and Optics*. 2014. 3 (91)
5. Epps B.P. Review of Vortex Identification Methods // 55th AIAA Aerospace Sciences Meeting. 2017. AIAA 2017-0989. DOI: 10.2514/6.2017-0989
6. Liu C., Gao Y., Dong X., Wang Y., Liu J., Zhang Y., Cai X., Gui N. / Third generation of vortex identification methods: Omega and Liutex/Rortex based systems // *J. Hydrodyn.* 2019. 31 2, pp. 205–223.
7. Shrestha P., Nottage C., Yu Y., Alvarez O., Liu C. / Stretching and shearing contamination analysis for Liutex and other vortex identification methods // *Advances in Aerodynamics*. 2021. 3 8.
8. Liu J., Liu C. Modified normalized Rortex/vortex identification method // *Phys. Fluids*. 2019. 31:061704, 6 p.
9. Kolář V., Šístek J. Stretching response of Rortex and other vortex-identification schemes // *AIP Advances*. 2019. 9, 105025. DOI: 10.1063/1.5127178
10. Keldysh Institute of Applied Mathematics, Russian Academy of Sciences, Shared Use Center // <https://ckp.kiam.ru/?home>
11. ARES software package for calculating three-dimensional turbulent flows of viscous compressible gas on high-performance computing systems. V.E. Borisov, A.A. Davydov, I.Yu. Kudryashov, A.E. Lutsky. Certificate of registration of the computer program RU 2019667338, December 23, 2019
12. V.E. Borisov, A.A. Davydov, I.Yu. Kudryashov, A.E. Lutsky, I.S. Men'shov. Parallel Implementation of an Implicit Scheme Based on the LU-SGS Method for 3D Turbulent Flows // *Mathematical Models and Computer Simulations*, 2015, 7 (3), p. 222–232.
13. Allmaras S.R., Johnson F.T., Spalart P.R.. Modifications and Clarifications for the Implementation of the Spalart-Allmaras Turbulence Model // *Seventh International Conference on CFD (ICCFD7)*, Big Island, Hawaii, 9-13 July 2012.
14. Computing complex K-60 // <https://www.kiam.ru/MVS/resources/k60.html> .
15. Liu C., Gao Y., Tian S., Dong X. Rortex—A new vortex vector definition and vorticity tensor and vector decompositions // *Phys. Fluids*. 2018. 30:035103.
16. Garth Ch., Tricoche X., Salzbrunn T., Bobach T., Scheuermann G. Surface techniques for vortex visualization // *VISSYM'04: Proceedings of the Sixth Joint Eurographics - IEEE TCVG conference on Visualization*, Konstanz Germany, May 19-21, 2004. pp. 155-164.
17. Canivete Cuissa J.R., Steiner O. Innovative and automated method for vortex identification – I. Description of the SWIRL algorithm // *A&A* 668. 2022. A118, doi: 10.1051/0004-6361/202243740.
18. Jeong J., Hussain F. On the identification of a vortex // *Journal of Fluid Mechanics*. 1995. Volume 285, pp. 69–94.
19. Hunt J.C.R., Wray A.A., Moin P. Eddies, stream, and convergence zones in turbulent flows // *Technical Report N° CTR-S88*. Palo Alto: Center for Turbulent Research. 1988. pp 193–208.